Quantum Electronics **51** (11) 1009–1018 (2021)

INTERACTION OF LASER RADIATION WITH MATTER. LASER PLASMA https://doi.org/10.1070/QEL17644

Cumulation and mixing of ions in a tubular focus of a high-power laser pulse

V.F. Kovalev, V.Yu. Bychenkov

Abstract. **As applied to laser acceleration of ions, we have constructed an analytical solution to the Cauchy problem for the kinetic equation, which describes the radial motion of particles under the action of a ponderomotive force in a tubular focus of a high-power laser beam propagating in a transparent plasma. For axisymmetric geometry, we have obtained the time and spatial dependences of the ion distribution function and have found their integral characteristics, such as density, average velocity, and energy spectrum. The appearance of ion density peaks inside the laser caustics, the cumulation of ions on the axis, and the effect of the formation of a multi-flux regime of ion motion are described analytically. The efficiency of the generation of neutron bursts by a laser pulse in the focal region in the case of cylindrical cumulation of ions is estimated.**

Keywords: *laser acceleration of ions, cumulation of ions, multiflux regime, tubular laser beam, neutron generation.*

1. Introduction

Among the widely discussed schemes for the generation of high-energy ions by an intense laser pulse, the scheme of radial ion acceleration from a laser-plasma channel formed during the propagation of the light in a transparent plasma of subcritical density is often considered [1–8]. Laser-accelerated ions from a low-density plasma are interesting from the point of view of their use for obtaining neutrons and various radionuclides, including medical ones [2, 9–11].

The dynamics of the radial acceleration of ions by laser radiation in a low-density plasma formed in targets such as, for example, a gas jet [2], evaporated foil [12], and nanoporous carbon [13], is largely due to the ponderomotive action of a laser pulse on plasma electrons. The latter are pushed out by the ponderomotive force from the region with a high laser-intensity gradient, resulting in the formation of a channel with a strong radial electric field of charge separation, which accelerates the ions. The problem of ion acceleration considered in [3, 6] served as a convincing example of the fact that the analytical description of particle acceleration by a laser pulse from a plasma channel formed in the caustic region or arising as a result of self-focusing is a challenging task even for approximate approaches. Therefore, the existing theoretical models [3, 4, 6] only very qualitatively characterise the radial acceleration of particles from the laser-plasma channel. Consequently, the spatiotemporal distribution of laser-accelerated particles is investigated mainly by kinetic numerical modelling techniques, usually by the particle-in-cell (PIC) method [14–16]. Some simplification is introduced by the numerical one-dimensional electrostatic model of ponderomotive acceleration, describing the dynamics of radial plasma expansion under the action of a given field [3, 6], when only the slow dynamics of plasma electrons is taken into account, which corresponds to averaging over their fast oscillations in the laser field. Based on numerical simulations, Sarkisov et al. [3] and Macchi et al. [6] found that electrons quickly respond to the ponderomotive action of the laser radiation, so that the electric field in the channel is determined with a good degree of accuracy by the condition for the balance between the electrostatic force that returns electrons to the channel and the ponderomotive force that pushes them out. While such a balance exists, the dynamics of ion acceleration can be studied rigorously analytically using the kinetic equation for ions with a given electrostatic field, which was implemented in [7, 8] for a cylindrical laser beam.

Note that the authors of Refs [3–8] discussed laser beams with an intensity that had a maximum on the beam axis and decreased monotonically with increasing radius, which led to the acceleration of ions from the axis of the laser beam to its periphery. This monotonic distribution of the laser beam intensity is not the only interesting configuration for ion acceleration. Along with it, another configuration is discussed, that is, a tubular one of a laser beam with an intensity maximum, which is located at a finite distance from the beam axis (ring) [2, 17–19]. It provides the cumulation of accelerated ions on the axis, which, in particular, can be realised using Bessel–Gaussian beams (see, for example, [20, 21]). Such cumulation can be more effective than simple irradiation of a cylindrical cavity with a laser pulse [17]. Focusing the laser beam into a ring-shaped spot leads to the fact that some of the ions located on the inner side of the ring experience radial acceleration towards the centre and form a converging collisionless cylindrical shock wave. Some time later, fast ions cumulate on the axis of the laser beam with the formation of a high-density plasma filament from interpenetrating ion fluxes with a small (compared to the ring diameter) transverse size and a length comparable to the length of the laser radia-

V.F. Kovalev Keldysh Institute of Applied Mathematics, Russian Academy of Sciences, Miusskaya pl. 4, 125047 Moscow, Russia; Centre for Fundamental and Applied Research, Dukhov Automatics Research Institute (VNIIA), ul. Sushchevskaya 22, 127055 Moscow, Russia; e-mail: vfkvvfkv@gmail.com;
V.Yu. Bychenkov Lebedev Physical Institute, Russian Academy of Sciences, Leninsky prosp. 53, 119991 Moscow, Russia; Centre for Fundamental and Applied Research, Dukhov Automatics Research Institute (VNIIA), ul. Sushchevskaya 22, 127055 Moscow, Russia; e-mail: bychenk@sci.lebedev.ru

Received 3 August 2021
Kvantovaya Elektronika **51** (11) 1009–1018 (2021)
Translated by I.A. Ulitkin

tion caustic. Such cumulation opens up opportunities for the efficient implementation of nuclear reactions, the rate of which is proportional to the product of the densities of the colliding particles. In this case, the ion energy can be controlled by changing the size of the focusing ring, the intensity distribution at the focus, as well as the laser radiation energy and duration. To optimise the proposed scheme of ion acceleration by a tubular laser beam and select the desired parameters to obtain a maximum reaction yield, it is important to construct an analytical model of the ion cumulation effect, which, although previously discussed [19, 22], has not yet been described. The latter is the main goal of our work, which represents the development of a simpler theoretical approach [7] as applied to the study of the dynamics of ion acceleration in the case of tubular laser beam geometry.

2. Kinetic model of ponderomotive acceleration of ions

Let us consider a cylindrically symmetric tubular laser beam in a transparent plasma. The inhomogeneity of the electric laser field along the radius leads to the displacement of plasma electrons from the region of the action of a strong electric field, that is, to the appearance of inhomogeneity of the electron density and the charge separation field, which, in turn, causes a redistribution of the ion density and the acceleration of ions to high energies in the radial direction. The dynamics of this process can be described using kinetic equations for the distribution functions of plasma electrons and ions, and the effect of the electric field is taken into account in the kinetic equation for electrons in the form of an additional electrostatic force that specifies the action of the ponderomotive force averaged over the high frequency of the laser field [23, 24]. However, as shown by the results of numerical simulations [6], until significant temperature gradients appear in the plasma and there occurs the breaking of the radial profile of the ion flux, the electric field in the plasma in the beam propagation region is determined by the balance condition for the electrostatic force, $-e\boldsymbol{E}$, which returns electrons into the channel, and the ponderomotive force that pushes them out, $\boldsymbol{F}_{\rm p} = -mc^2\nabla\sqrt{1+a^2/2}$ (a is the standard dimensionless vector potential of the laser field), that is, $e\boldsymbol{E} = \boldsymbol{F}_{\rm p}$. This is quite natural due to the small mass of electrons, which, while rapidly oscillating at the laser and plasma frequencies, tend to establish such an equilibrium state. In this case, it is also assumed that the intrinsic electron pressure is small in comparison with the light pressure.

Taking this fact into account, it is possible to greatly simplify the mathematical model describing the acceleration of ions, leaving only the kinetic equation for ions, in which the electric field is assumed to be specified. Taking into account the symmetry of the laser beam propagating along the z axis, we will consider the ion kinetic equation for the ion distribution function integrated over the longitudinal and axial velocity components in the cylindrical coordinate system $\{r, \varphi, z\}$ with allowance for its dependence only on time t, radial coordinate r and radial component $v_{\rm r}$ of the ion velocity. As a result, we arrive at the Cauchy problem for the kinetic equation for the ion distribution function of plasma particles $f^{\rm i}(\tau, x, v)$ integrated over v_φ and $v_{\rm z}$ (for definiteness, we neglect the thermal spread in velocities v_φ and $v_{\rm z}$):

$$\partial_\tau \tilde{f} + v\partial_x \tilde{f} + p\partial_v \tilde{f} = 0,\ \tilde{f} = xf,\ \ p = p(\tau, x),$$
$$f|_{\tau=0} = f_0(x, v). \tag{1}$$

Here $\tau = \omega_{\rm Li}t$ is the dimensionless time; $\omega_{\rm Li}$ is the Langmuir frequency of ions with mass $M_{\rm i} = AM$ and charge $e^{\rm i} = Ze$; A and Z are the mass and charge numbers of ions; M is the proton mass; $x = r/R$ is the dimensionless coordinate; R is the characteristic spatial scale of the localisation of the laser intensity along the radius; $v = v_{\rm r}/(\omega_{\rm Li}R)$ is the dimensionless ion velocity; $p = ZeE/(M_{\rm i}R\omega_{\rm Li}^2)$ is the dimensionless electric field; $f^{\rm i} = [n_0/(\omega_{\rm Li}R)]f$ is the dimensionless distribution function of ions; and n_0 is the unperturbed ion density. In expression (1), the choice of the normalisation $f^{\rm i}$ to the characteristic ion velocity $\omega_{\rm Li}R$, rather than to the typically used thermal velocity, is due to the fact that in the formulation of the problem discussed here, the thermal spread of ions in velocities is insignificant and, therefore, the thermal velocity of ions is small in comparison with the value of $\omega_{\rm Li}R$ used for normalisation.

Taking into account the relationship between the electric field in plasma and the laser intensity gradient, the expression for the electric field takes the form

$$p = -\frac{c^2}{\omega_{\rm Le}^2 R^2}\partial_x\sqrt{1 + a^2(\tau, x)/2}\,. \tag{2}$$

Here $\omega_{\rm Le}$ is the Langmuir frequency of electrons with mass m and charge $e^{\rm e} = -e$; $a^2(\tau, x) = A(\tau)a^2(x)$ characterises the dimensionless intensity (energy flux density) of laser radiation; $a^2(x) = a_0^2 I_0(x, a_0^2)$; $a_0 = 0.85\times10^{-9}\lambda\sqrt{I_{00}}$; λ is the wavelength of laser radiation (μm); I_{00} is the intensity (energy flux density) of the laser pulse at maximum (W cm^{-2}); and the function $A(\tau)$ is the laser pulse envelope. The function $a^2(x)$ characterises the distribution of the laser intensity along the radius; for example, for a laser beam with a monotonic decrease in intensity with distance from the axis [6] the variant with $I_0 = \exp(-x^2)$ was used in numerical calculations, and for a tubular laser beam [2] the intensity distribution along the radius in dimensional variables was set in the form $I_0 = (r/r_0)^4\exp[2 - 2(r/r_0)^2]$, where r_0 is the radius of the tubular beam related to the focal spot size $2R_{\rm las}$ (according to the position of the intensity maximum) by the expression $R_{\rm las} = r_0$. In the dimensionless variables used by us, this distribution of the tubular beam intensity takes the form

$$I_0 = (x/b)^4\exp[2 - 2(x/b)^2], \tag{3}$$

where $b = r_0/R$ is the dimensionless radius that specifies the position of the maximum intensity of the tubular beam.

When studying equations of form (1), use is conventionally made of the method of characteristics. This equation is most simply studied for a time-independent electric field, $p = p(x)$, which corresponds to the quasi-stationary regime, in which the laser pulse duration exceeds the characteristic time of ion acceleration. In this case, the characteristics of Eqn (1) are integrated and its solution $\tilde{f} = F(j_1, j_2)$ is written in terms of the invariants j_1 and j_2

$$j_1 = v^2/2 - \Phi,\ \ j_2 = \tau - \int\frac{{\rm d}\Phi}{\Psi(\Phi)\sqrt{2(j_1 + \Phi)}}, \tag{4}$$

where the potential Φ and the function $\Psi(\Phi)$ are related by implicit expressions

$$p(x) = \partial_x\Phi = \Psi(\Phi). \tag{5}$$

For a detailed understanding of the ion acceleration process, of greatest interest is the case when integrals (4) are calculated explicitly. This is realised with a special specification of the spatial distribution of the electric field p, which, nevertheless, must correspond to the physically justified profile of the laser intensity of the tubular beam. Let us consider a simple example of calculating invariants and writing the solution of the kinetic equation (1) for a radially localised electric field distribution of the form

$$p = \rho \tanh y \cosh^{-2} y, \quad \rho = \frac{2c^2}{\omega_{Le}^2 R^2}(\sqrt{1 + a_0^2/2} - 1), \qquad x - b = y. \tag{6}$$

Due to the cylindrical symmetry of the problem, the electric field at the beam centre ($x = 0$) should vanish, which for the above electric field is satisfied with an exponentially small error at $b \gg 1$. Formally, the condition $p|_{x=0} = 0$ can be exactly satisfied for the potential $\tilde{\Phi} = \Phi[1 - \exp(-\alpha^2 x^2)]$, $\alpha \gg 1$, differing from Φ by an additional factor, which coincides with unity everywhere except in a small vicinity of zero, $x \ll 1/\alpha$. In what follows, the difference between Φ and $\tilde{\Phi}$ for $b \gg 1$ will be neglected, considering it exponentially small. Dependence (6) of the electric field on the coordinate x corresponds to a linear change with increasing $|y|$ of the electric field in the plasma cylinder at $|y| \ll 1$ and to its exponential decay at large radii $|y| \gg 1$. The electric field in (6) can be represented, as in (2), in the form of the spatial gradient of the potential of the electric field generated by the ponderomotive force,

$$p = -\frac{\rho}{2}\partial_x \cosh^{-2} y. \tag{7}$$

Comparison of (2) with (7) implies that the intensity of laser radiation, which is formed by an electric field (6), has the form

$$a^2(x) = 2\{[1 + (\sqrt{1 + a_0^2/2} - 1)\cosh^{-2} y]^2 - 1\}. \tag{8}$$

The chosen dependence (8) is also characterised by a monotonic decrease in the intensity $I_0(x, a_0^2)$, typical for a tubular beam, with distance in both directions from the maximum localised at point $x = b$, $I_0(b, a_0^2) = 1$.

The use of (6) in (4) generates a solution to the kinetic equation (1) of the form:

$$\tilde{f} = F(\check{x}, \check{v}), \tilde{\tau} = \tau\sqrt{\rho}\sqrt{v^2 + \cosh^{-2} y}, v^2 = v^2/\rho,$$

$$\sinh \check{y} = \sinh y \cosh \tilde{\tau} - v \cosh y \sinh \tilde{\tau}/\sqrt{v^2 + \cosh^{-2} y}, \tag{9}$$

$$\check{v} \cosh \check{y} = v \cosh y \cosh \tilde{\tau} - \sqrt{v^2 + \cosh^{-2} y} \sinh y \sinh \tilde{\tau}.$$

For a negligibly low ion temperature (the limit of cold ions) and a uniform initial ion density, we have $F_{|\tau=0} = n_0\delta(v)$, and solution (9) is written in the form

$$f = n_0 \frac{\check{x}}{x}\delta(\sqrt{\rho}\check{v}). \tag{10}$$

Multiplying (10) by unity and v as well as integrating over v, we obtain expressions for the integral characteristics of ions with distribution function (10) – their density and average velocity,

$$n_{av} = n_0 \sum_k \frac{\check{x}_k}{x} \{|\partial_v \check{v}_{|x=\text{const}}|^{-1}\}_{|v=v_k},$$

$$v_{av} = \frac{n_0}{n_{av}} \sum_k \frac{\check{x}_k}{x}\sqrt{\rho}\,\check{v}_k \{|\partial_v \check{v}_{|x=\text{const}}|^{-1}\}_{|v=v_k}. \tag{11}$$

Here $\check{x}_k = \check{x}(x, v_k)$ and the summation is performed over all values of the roots v_k of the equation $\check{v} = 0$, which in the variables y, v has a simple form:

$$v/\sqrt{v^2 + \cosh^{-2} y} - \tanh y \tanh(\tilde{\tau}\sqrt{v^2 + \cosh^{-2} y}) = 0, \qquad \tilde{\tau} = \tau\sqrt{\rho}. \tag{12}$$

It is easy to verify that equation (12) does not change when v is replaced by $-v$ and y by $-y$, that is, the curves on the phase plane $\{y, v\}$ are symmetric with respect to point $y = 0$, $v = 0$. The ions lying in regions with $y > 0$ (at $x > b$) are accelerated by the electric field into the outer region of the tubular beam. Ions located in the inner region of the tubular beam $-b < y < 0$ (at $0 < x < b$) are accelerated towards its axis. This situation persists at least until a certain time instant $\tau = \tau_c$, which is determined from the condition that the ions accelerated inside the shell of the tubular beam reach its axis. The graphs of the curves $\check{v} = 0$ on the phase plane $\{y, v\}$ for $-b < y < \infty$ at various times $\tilde{\tau} < \tau_c$ are shown in Fig. 1 for $b = 10$.

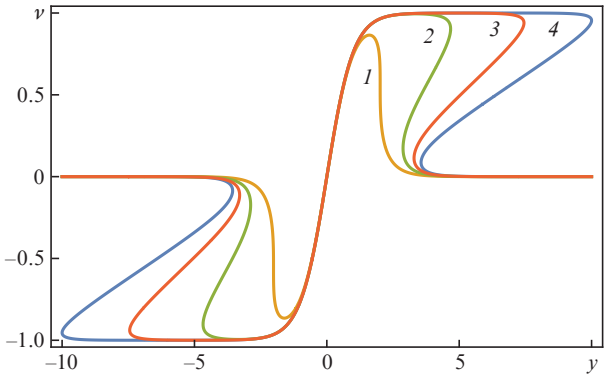

Figure 1. Graphs of curves $v = v(y)$ on the phase plane $\{y, v\}$ for the instants of time: (*1*) $\tilde{\tau} = \tilde{\tau}_* \approx 2.78989$ (the moment of the breaking of the ion velocity profile with the formation of a three-flux regime), (*4*) $\tilde{\tau} = \tilde{\tau}_c \approx 11.6955$ (the moment of the onset of ion cumulation in the inner region on the beam axis $y = -b = -10$), and (*2*) $\tilde{\tau} = 6$ and (*3*) $\tilde{\tau} = 9$ (intermediate values of time).

The behaviour of the curves on the phase plane in the outer region, $y > 0$, actually repeats (after replacing x with y) the results of [7]. It follows from them that at large times $\tilde{\tau} > \tilde{\tau}_*$ the dependence $v(y)$ is not unambiguous in the entire range of variation of the variable y and resembles, for example, the velocity profile in a Coulomb plasma explosion [25], which demonstrates the overtaking of peripheral particles by internal particles that are in a stronger accelerating field. The upper y_{up} and lower y_{low} boundaries of the domains of multivaluedness of the solution $y_{low} < |y| < y_{up}$ are determined by the condition that the derivative of the inverse function $\partial_v y = 0$ vanishes, which leads to the following two equations for the coordinates of the boundaries:

$$\tilde{\tau}v - \omega\tanh y\tanh\omega = 0,$$

$$\omega - \tilde{\tau}v\tanh y(\tanh\omega + \omega\cosh^{-2}\omega) = 0, \qquad (13)$$

$$\omega = \tilde{\tau}\sqrt{v^2 + \cosh^{-2}y}\,.$$

The moment $\tilde{\tau}_*$ of the emergence of a multiflux (three-flux) regime is found from the conditions for the simultaneous vanishing of the derivatives $\partial_v y = \partial_{vv} y = 0$. These conditions are written in the form of three equations combining (13) and the equation

$$\cosh^2\omega_*\tanh\omega_* + \omega_*[1 + 2\cosh^2 y_* v_*^2(1 - \omega_*\tanh\omega_*)] = 0, \qquad (14)$$

$$\omega_* = \tilde{\tau}_*\sqrt{v_*^2 + \cosh^{-2}y_*}\,.$$

Numerical solution of equations (13) and (14) yields 'universal' (that is, valid for any value of ρ and b, taking into account $b \gg 1$) values $\tilde{\tau}_* \approx 2.78989$, $y_* \approx \pm 2.01412$, and $v_* \approx \pm 0.55715$. Here, the plus sign corresponds to the outer region of the tubular beam ($y > 0$), and the minus sign corresponds to the inner (axial) region of the tubular beam ($-b < y < 0$).

For $\tilde{\tau} > \tilde{\tau}_*$ and $y > 0$, or, which is the same, $x > b$, three values of the variable $v = v_1$, v_2 or v_3 corresponds to each y_i from the region $y_{\rm low} < y < y_{\rm up}$. At the upper and lower boundaries of the domain of multivaluedness, $y = y_{\rm low}$ and $y_{\rm up}$, two of the three roots merge.

For the inner region of a tubular beam ($-b < y < 0$), the pattern of curves on the phase plane is more complex, taking into account additional space–time constraints. First, the breaking of the ion flux upon cumulation of ions onto the axis, which occurs at $\tilde{\tau} = \tilde{\tau}_*$, implies that the moment of breaking is reached before the ions cross the beam axis, that is, the coordinate of the breaking point $y_* > -b$.

Taking into account the initial assumption about the exponential smallness of the electric field on the beam axis, the last condition is satisfied with a margin, $|y_*| \ll b$. Second, the difference in the behaviour of ions in the inner region from the three-flux region in the outer region begins to manifest itself when ions accelerated by the electric field of the inner part of the shell of the tubular beam cross the beam axis. The instant $\tilde{\tau}_{\rm c}$ of reaching the beam axis by the ions and the velocity $v_{\rm c} < 0$ at this instant are found from the condition that the boundary of the three-flux flow specified by Eqns (13) coincides with the beam axis $y = -b$, that is $x = 0$:

$$\tilde{\tau}_{\rm c} = \omega_{\rm c}\cosh b(1 - \tanh^2 b\tanh^2\omega_{\rm c})^{1/2},$$

$$v_{\rm c}^2 = \tanh^2\omega_{\rm c}\frac{\tanh^2 b(1 - \tanh^2 b)}{1 - \tanh^2 b\tanh^2\omega_{\rm c}}, \qquad (15)$$

$$1 - \omega_{\rm c}\tanh\omega_{\rm c}\tanh^2 b + (\omega_{\rm c}\tanh\omega_{\rm c} - 1)\tanh^2 b\tanh^2\omega_{\rm c} = 0.$$

The change in the position of the boundaries of the three-flux flow with time $\tilde{\tau}$ after the breaking and up to the moment of cumulation onto the axis, $\tilde{\tau}_{\rm c} > \tilde{\tau} > \tilde{\tau}_*$, is shown in Fig. 2a.

To study the behaviour of the kinetic equation after cumulation of ions onto the axis, it is necessary to understand the processes of crossing the beam axis by ions and their further evolution in a decelerating electric field. Since, due to the cylindrical symmetry of the problem, the electric field vanishes on the axis of the laser beam, its intersection by ions is

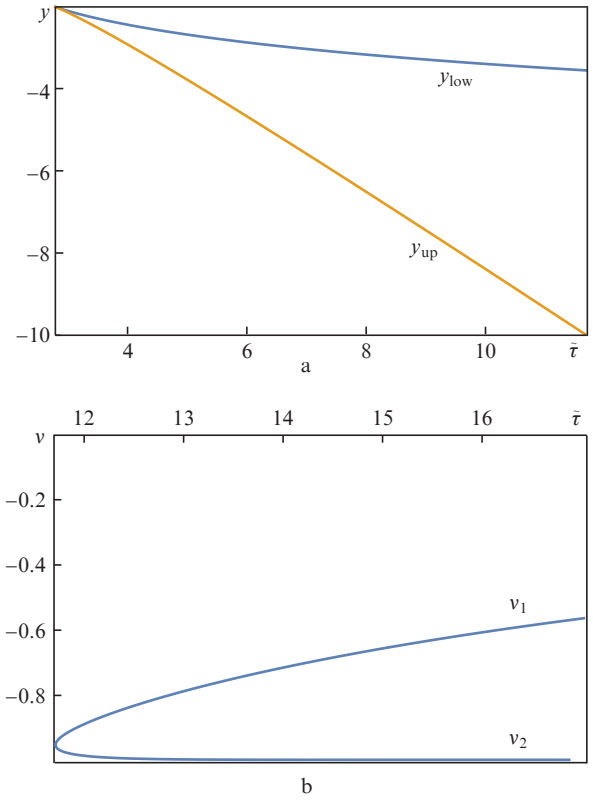

Figure 2. (a) Coordinates of the boundaries $y_{\rm up}$, $y_{\rm low} < 0$ of the three-flux flow zone, $y_{\rm up} < y < y_{\rm low}$, for the inner region of the tubular beam $-b < y < 0$ at $b = 10$ and $\tilde{\tau}_* \leqslant \tilde{\tau} \leqslant \tilde{\tau}_{\rm c}$, $\tilde{\tau}_* \approx 2.78989$, and $\tilde{\tau}_{\rm c} \approx 11.6955$, as well as (b) the velocities of ions, $v_{1,2} < 0$, reaching the axis in the inner region of the tubular beam at $\tilde{\tau} > \tilde{\tau}_{\rm c} \approx 11.6955$, as functions of time $\tilde{\tau}$.

equivalent to the appearance of ions reflected from the axis, the dynamics of which can be considered on the basis of solving the 'initial-value' problem for ions located at the initial moment (determined by the time of cumulation on the axis) on the beam axis and having a velocity directed from the beam axis. We emphasise that the process of cumulation on the beam axis does not occur simultaneously for different groups of ions: ions located at the boundary of the three-flux flow are the first to be there. With increasing time $\tau > \tau_{\rm c}$, the beam axis is reached by the ions with velocities both higher and lower than $v_{\rm c}$. The range of these velocities at $\tau > \tau_{\rm c}$ is characterised by the lowest $v_2 < 0$ and highest $v_1 < 0$ (in absolute value) velocities and is given by solving equations of form (12), in which we set $y = -b$:

$$\frac{v_{1,2}}{\sqrt{v_{1,2}^2 + \cosh^{-2}b}} + \tanh b\tanh(\tilde{\tau}\sqrt{v_{1,2}^2 + \cosh^{-2}b}) = 0. \qquad (16)$$

After reflection from the axis, the ions form a cloud of ions flying from it in a decelerating electric field: their movement in the axial region of the beam becomes five-flux. The analytical solution of the boundary value problem for reflected ions is obtained, as before, using the first integrals for the kinetic equation (1). The 'initial' conditions are set by the positive (that is, directed from the beam axis) ion velocity, $|v_{\rm a}| > 0$, on the beam axis, $y = -b$, after reflection at time $\tilde{\tau} = \tilde{\tau}_{\rm a}$. The ion velocities before reflection (that is, directed to the beam axis) are found from the equation of form (16) with $v_{1,2}$ replaced by $v_{\rm a}$, and the position of point $\breve{y}_{\rm st}$, from which

ions come to the axis with a velocity $v_a < 0$, is given by the expression

$$\sinh \breve{y}_{st} = -\sinh b \cosh \omega_a - \frac{v_a \cosh b \sinh \omega_a}{\sqrt{v_a^2 + \cosh^{-2} b}},$$
$$\omega_a = \tilde{\tau}_a \sqrt{v_a^2 + \cosh^{-2} b}\,. \tag{17}$$

In particular, assuming $\tilde{\tau}_a = \tilde{\tau}_c$, we obtain $\sinh \breve{y}_{st} = -\sinh b/\cosh \omega_c$. Further solving the boundary value problem of deceleration for reflected ions with an initial velocity $|v_c| > 0$, we find that the ions stop at a point with a coordinate coinciding with the starting point, from where the acceleration process began, and the deceleration time is equal to $\tilde{\tau}_c$. After that, the process is repeated with the formation of a seven-flux ion flow in the paraxial region. The characteristic spread in the velocities of the ions involved in the multiflux movement can be estimated by plotting the dependences of the velocities $v_{1,2}$ as a function of time $\tilde{\tau}$ (Fig. 2b). From the analysis of these dependences it follows that, in addition to the ions that have reached the beam axis at the instant $\tilde{\tau} = \tilde{\tau}_c$, during the characteristic time of their subsequent deceleration (of the order of $\tilde{\tau}_c$), other ions will reach the beam axis, the velocities of which lie in the range from v_2 to v_1, that is the value of the spread in ion velocities $|v_1 - v_2|$ is comparable to v_c, which indicates a rapid chaotisation of the ion dynamics in the paraxial region.

3. Global characteristics of ions

The presence of multiflux flow regions is clearly manifested in global characteristics of ions. These are the average characteristics of accelerated ions, calculated by integrating [by summation in the case of (10)] the distribution function of ions over their velocities, namely: the average density and velocity, as well as the spectrum of ions. Crossing the boundary of the multivaluedness domain is accompanied by a jump-like change in the number of particles contributing to the ionic moments, that is, to the density and velocity, which leads to corresponding discontinuities in these characteristics.

The use of (12) in (11) leads to a simpler form of the relations that determine the density and average velocity of ions:

$$n_{av} = n_0 \sum_k \frac{1}{x}\left[b + \operatorname{arcsinh}\left(\frac{\sinh y}{\cosh \omega_k}\right)\right] |\,\partial_v \breve{v}_{|v = v_k}\,|^{-1},$$
$$v_{av} = \frac{n_0}{n_{av}} \sum_k \frac{v_k}{x}\left[b + \operatorname{arcsinh}\left(\frac{\sinh y}{\cosh \omega_k}\right)\right] |\,\partial_v \breve{v}_{|v = v_k}\,|^{-1}, \tag{18}$$
$$\partial_v \breve{v}_{|\breve{v} = 0} = \frac{\cosh y}{\sqrt{\sinh^2 y + \cosh^2 \omega}}$$
$$\times [\cosh^2 \omega - \tanh^2 y (\sinh^2 \omega + \omega \tanh \omega)].$$

As illustrations of formulae (18), Fig. 3 shows typical curves of ion density distributions for four moments of time, the first of which corresponds to the beginning of the breaking of the ion flux, and three subsequent ones belong to the region of existence of a multiflux (in this case, three-flux) flow.

The transition to a multiflux (three-flux) regime is accompanied by the expected formation of singularities in the distribution of the ion density, similar to those observed during the evolution of ions in the field of a laser beam with a monotonically decreasing intensity with distance from its axis [7, 8], as well as those that have been repeatedly discussed in various works related to the emergence of multiflux motions in the study of the dynamics of noninteracting particles [26], in the analysis of the dynamics of a nondissipative gas in an expand-

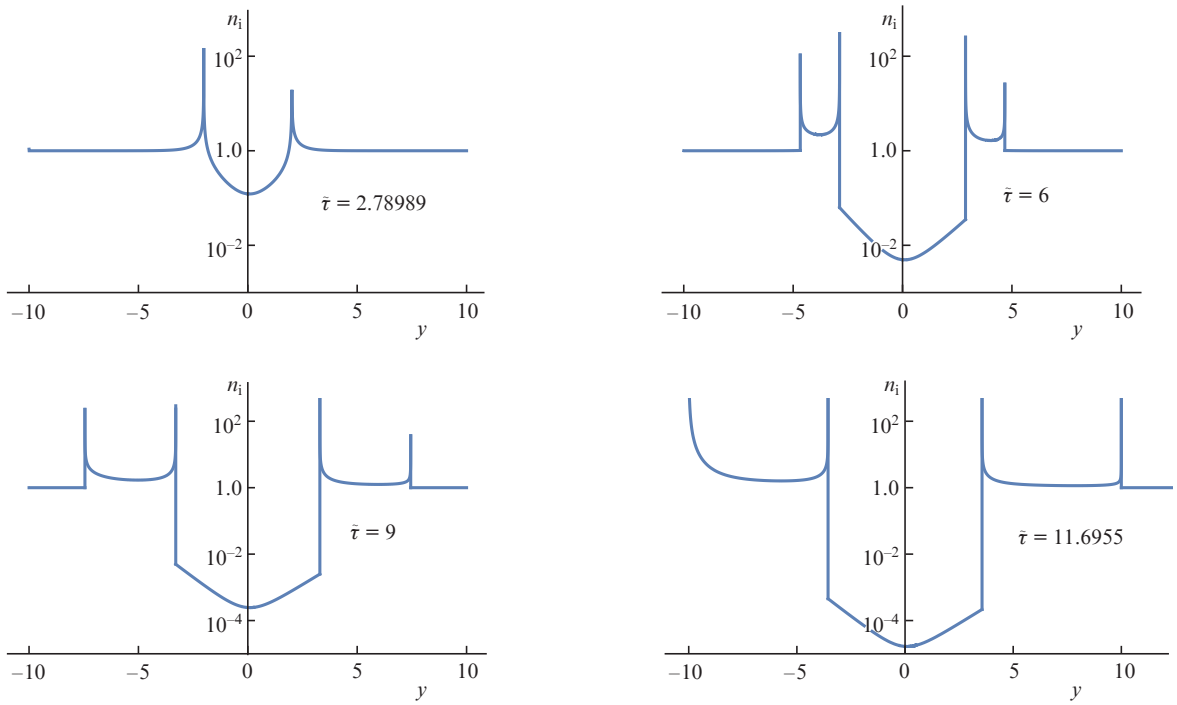

Figure 3. Spatial distribution of the ion density along the x coordinate for the same instants of time as in Fig. 1; $b = 10$.

ing universe [27], and in problems of a Coulomb plasma explosion (see, for example, [25, 28]). Note that the distance between the ion density peaks in the outer region, where the dynamics of ions is similar to their dynamics for a beam with a maximum intensity on the axis [7], also grows rapidly with time, and the peaks themselves have a small width. This can be understood from the analysis of the graphs of the curve $\check{v} = 0$ on the phase plane $\{y, v\}$: regions where the derivative $\partial_v y$ is small, which corresponds to large values of the average ion density, are characterised by a small range of variation of the y coordinate, and with increasing time the width of such regions decreases. This is especially noticeable for the peak that is farther away from the position of the maximum intensity of the tubular beam.

A different situation is observed in the inner region of the tubular beam: of the two density peaks, the largest width is at the peak that is farther away from the position of the maximum intensity of the tubular beam. The width of this first peak moving towards the beam axis increases with time and turns out to be maximum by the time the ions are cumulated onto the beam axis, that is, a significant fraction of the ions in the inner region is localised in the vicinity of the beam axis. The width of the second peak of ion density moving towards the beam axis turns out to be significantly narrower, and the number of ions in its vicinity is small in comparison with the first peak. This structure is well observed in a numerical experiment with a tubular laser beam [2]. In Fig. 1 in paper [2], in the inner region after the breaking of the ion profile, one can clearly see the formation of two ion density peaks, the first of which broadens as it approaches the beam axis, reaching the largest width at the moment of cumulation on the axis. The phenomenon of reflection of ions from the axis with the formation of a bunch of reflected ions is also observed. From the second peak, only its pedestal is visually observed, since the very small width of the ion density peak makes it difficult to detect its central region in numerical calculations.

Similarly to how it was done for the average ion density, one can use (18) to construct graphs of the average ion velocity, which, as in the case of beam expansion with a maximum intensity on the axis, will also have discontinuities at the intersection of the boundaries of the regions of existence of multiflux flows. However, we will not dwell on this here, referring the reader to the previously obtained results for a cylindrical beam with a monotonically decreasing intensity [7].

In addition to formulae (18), which specify the spatial distribution of the average ion velocity and their density, of interest are also formulae that determine the energy spectrum of accelerated ions, N_ε. The integral of N_ε over all admissible values of the ion energies $0 < \varepsilon < \infty$ coincides with the total number of plasma ions:

$$N_\varepsilon = \pi \int_0^\infty \mathrm{d}x x \sqrt{\frac{2}{\varepsilon}} [f(x, \sqrt{2\varepsilon}) + f(x, -\sqrt{2\varepsilon})]. \tag{19}$$

Substitution of (10) into (19) determines the spectrum of ions accelerated by the laser field:

$$N_\varepsilon = 2\pi \frac{n_0}{\sqrt{2\check{\varepsilon}}} \sum_k \left[b + \operatorname{arcsinh}\left(\frac{\sinh y}{\cosh \omega_k} \right) \right] | \partial_x \check{v}_{|x = x_k} |^{-1}, \; \check{\varepsilon} = v^2/2,$$

$$\partial_x \check{v}_{|\check{v}=0} = \frac{\tilde{\tau}}{\cosh y \sqrt{\sinh^2 y + \cosh^2 \omega}} \tag{20}$$

$$\times \left[\tanh^2 y - \cosh^2 \omega \frac{\tanh \omega}{\omega} (1 + v^2 - 2 \tanh^2 y) \right].$$

Here, in (20), the summation, in contrast to (18), is performed over all values of the roots x_k of the equation $\check{v} = 0$. The maximum value of the ion energy, the so-called energy cutoff, $\check{\varepsilon}_\mathrm{m} = v_\mathrm{m}^2/2$, at an arbitrary moment of time, is found from a system of two equations:

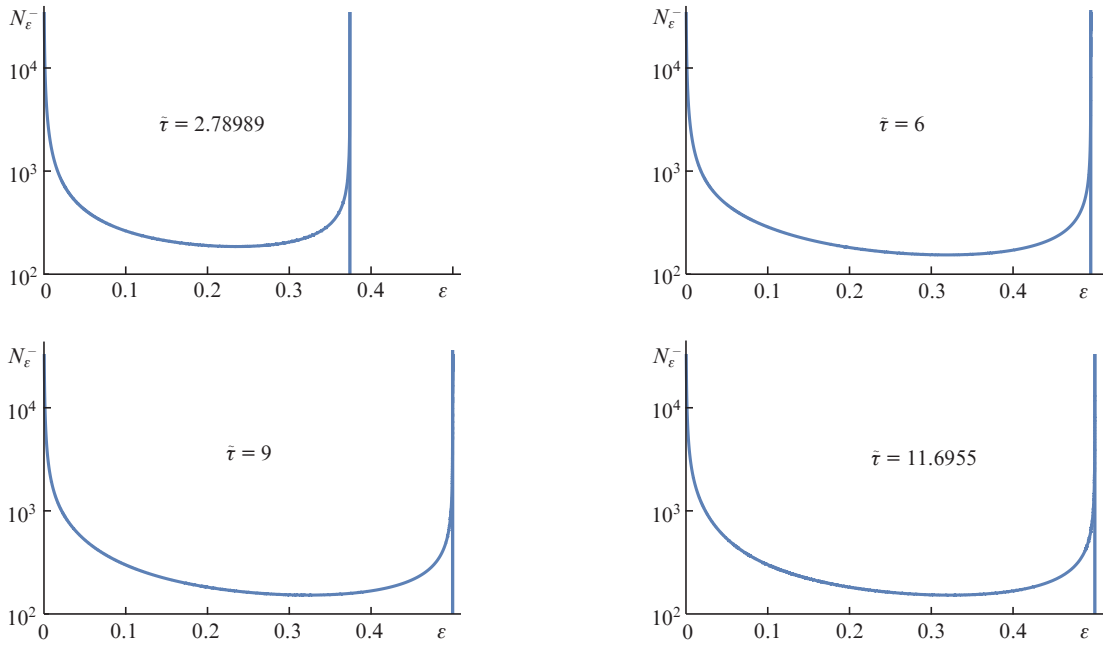

Figure 4. Spectrum of the ion energy distribution ε for the same instants of time as in Fig. 1. The minus sign in the notation for the spectral density N_ε^- means that these curves characterise the spectral distribution of ions only from the inner region, that is, those flying towards the beam axis.

$$\tilde{\tau}v_{\rm m} - \omega_{\rm m}\tanh y_{\rm m}\tanh\omega_{\rm m} = 0, \quad \omega_{\rm m} = \tilde{\tau}\sqrt{v_{\rm m}^2 + \cosh^{-2}y_{\rm m}}\,,$$
$$\omega_{\rm m}\tanh^2 y_{\rm m} - \cosh^2\omega_{\rm m}\tanh\omega_{\rm m}\left(1 + v_{\rm m}^2 - 2\tanh^2 y_{\rm m}\right) = 0. \tag{21}$$

A typical form of the spectral energy distribution of ions is shown in Fig. 4 for the same times as the spatial density distribution. The curves in Fig. 4 characterise the spectral distribution of ions only from the inner region, that is, those that fly towards the beam axis and are of greatest interest. It is seen that at $\tilde{\tau} \gtrsim 5$ the ion energy reaches its maximum value, $\check{\varepsilon}_{\rm m} \approx 1/2$, which virtually does not change with further growth of $\tilde{\tau}$. Note one feature of the spectral distribution of ions for a tubular beam, manifesting itself in a relatively smooth increase in N_{ε}^{-} near the upper boundary of the spectrum, which indicates the appearance of a noticeable fraction of high-energy ions during their acceleration. A similar shape of the spectral curves was also observed during ion acceleration by a super-Gaussian laser beam [9].

4. Discussion of the results and conclusions

The above-obtained results testify that the maximum value of the energy of the accelerated ions, $\check{\varepsilon}_{\rm m}$, does not exceed the value of 1/2, which is achieved in a time $\tilde{\tau}$, close to the time of occurrence of the multiflux motion $\tilde{\tau}_*$. This means that to achieve the maximum ion energy, the duration of the laser pulse $\tilde{\tau}_{\rm las}$ must be at least $\tilde{\tau}_*$. In dimensional variables, this constraint takes the form

$$t_{\rm las} \geqslant t_* = \sqrt{\frac{2}{3\sqrt{3}}}\frac{A}{Z}\frac{M}{m}\frac{R}{c}\frac{\tilde{\tau}_*}{\sqrt{p_{\max}}}, \tag{22}$$

where $p_{\max}$ is the maximum (in absolute magnitude) value of the normalised electric field amplitude $p_0(y)$ determined from the relation $p = (c^2/\omega_{\rm Le}^2 R^2)p_0$. For the discussed electric field (6), the extrema $p_0(y)$ [a maximum and a minimum of $p_0(y)$ in the outer and inner regions, respectively] and the value corresponding to these extrema

$$p_{\max} = \frac{2\rho}{3\sqrt{3}}\frac{\omega_{\rm Le}^2 R^2}{c^2} = \frac{4}{3\sqrt{3}}\left(\sqrt{1 + a_0^2/2} - 1\right) \tag{23}$$

are achieved when $y_{\max} = \operatorname{arcsinh}(1/\sqrt{2})$. Note that the number of extremum points of the electric field for a tubular beam is equal to two, in contrast to the version of a cylindrical beam with an intensity monotonically decreasing from the axis. Passing from $a_0 \ll 1$ to $a_0 \gg 1$, the quadratic dependence of $p_{\max} = (3\sqrt{3})^{-1}a_0^2$ on a_0 is replaced by a linear one: $p_{\max} = (2/3)^{3/2}a_0$. To calculate the time of cumulation of ions on the axis $t_{\rm c}$, $\tilde{\tau}_*$ should be replaced by $\tilde{\tau}_{\rm c}$ in (22).

By using the parameters of the laser and plasma, the maximum value of the ion energy in dimensional variables is written in the form

$$E_{\rm m} = \frac{3\sqrt{3}}{2}\check{\varepsilon}_{\rm m} Z p_{\max} mc^2, \tag{24}$$

which at $\check{\varepsilon}_{\rm m} = 1/2$ gives the upper estimate for the energy of accelerated ions $E_{\max} = 3\sqrt{3}\,p_{\max} Zmc^2/4$. At times shorter than that those required to achieve the maximum energy $\check{\varepsilon}_{\rm m} = 1/2$, the cutoff energy is found from equations (21).

Note that formula (22), as in the case of a cylindrical beam with a maximum intensity on the axis, is obviously universal in the sense that although a specific numerical value of $\tilde{\tau}_*$ is related to the details of the spatial structure of the electric field (2), the dependence of $p_{\max}$ on the intensity a_0^2 in (23) is the most important for determining the moment of the onset of the multiflux regime. In this case, one should expect adequate estimates of t_* using (22) for close spatial distributions of laser intensity.

As an example, we consider the cumulation of deuterons on the axis of a tubular laser beam with the parameters used in [2]: an intensity of 2×10^{19} W cm^{-2} and a laser pulse duration $t_{\rm las} \approx 400$ fs for irradiating gaseous deuterium with a density $n_{\rm D} \approx 10^{20}$ cm^{-3}. For characteristic scales $R \approx 1$ μm and $b = 10$, which corresponds to the radius of the laser spot in terms of maximum intensity $R_{\rm las} = bR = 10$ μm and the width of the ring at half maximum intensity –1.51 μm, from (22)–(24) we obtain $t_* \approx 0.28$ ps, $t_{\rm c} \approx 1.13$ ps and $E_{\max} \approx 1$ MeV.

It is interesting to compare the characteristic times and spatial scales of the electric field, which were obtained in this work, with similar values used in the numerical experiment [2]. For example, the maximum amplitude of the dimensionless electric field generated by a laser beam with intensity distribution (3) turns out to be about 4 times less than that given by formula (23), while the scale of its localisation along the radius is about 4 times larger. Indeed, the electric field analysed in our work (6) inside the ring has a maximum amplitude $p_{\max} \approx 1.54$ at $x \approx 9.532$ and falls off sharply at $x \lesssim 7$, that is, the ion acceleration zone is narrow and is located on the boundary of the inner region of the ring, and outside this zone ions fly by inertia. In [2], the situation is somewhat different: The amplitude of the electric field accelerating ions has a maximum of $p_{\max}^{\rm sar} \approx 0.377$ at $x \approx 5.45$, decreases when approaching the beam axis and is vanishingly small only in the paraxial region $x \lesssim 1.5$. This means that in the numerical experiment [2], ions are accelerated virtually in the entire inner region, with the exception of the narrow paraxial region of the beam. Since the amplitude of the accelerating electric field in [2] is four times smaller than that obtained by formula (23), the estimate of the characteristic breaking time of the ion flux according to (14) should be twice that given above, $t_*^{\rm sar} = 2t_* \approx 0.56$ ps, which corresponds to the estimates of work [2]. In this case, the cumulation time on the axis $t_{\rm c}^{\rm sar} \approx 1.2$ ps in [2] is twice $t_*^{\rm sar}$ and is comparable with the above $t_{\rm c} \approx 1.13$ ps, which may be due to the formation of a shock density wave immediately in the near-axis region, and therefore the time needed for it to reach the beam axis is less than that obtained for the density wave, which arises in the model discussed above at the boundary of the inner region of the ring. Finally, according to (24) for the conditions of the numerical experiment [2], an estimate of the maximum ion energy a $\check{\varepsilon}_{\rm m} = 1/2$ with allowance for a four times smaller amplitude of the accelerating electric field $p_{\max}^{\rm sar} \approx p_{\max}/4$ is $E_{\max}^{\rm sar} \approx 250$ keV, which also agrees with the results of [2].

Note that the employed model of ion dynamics in an accelerating field specified by the ponderomotive force of a tubular laser beam makes it possible to obtain spatiotemporal and spectral characteristics of accelerated ions. A limitation on the applicability of this model may be a violation of the balance between the strength of the electrostatic field of charge separation and the ponderomotive force of the laser beam, for example, due to an increase in the thermal pressure of electrons. A consistent approach to taking this effect into account is associated with the study of the kinetics of electrons and requires further additional studies using the com-

plete system of equations for the kinetics of plasma particles in a self-consistent field. These studies will serve as an additional justification for the statement that the breaking of the ion flux profile is not a significant limitation of the mathematical model if it occurs outside the region of localisation of a strong electric field of the laser beam, where ions move in a ballistic regime.

To summarise, we note that within the framework of the proposed model, we have analysed the behaviour of the ion distribution function as a function of the parameters of the plasma and the laser beam and have constructed the spatial distributions for the density of plasma ions for different instants of times. The spectral energy distribution of the accelerated ions and the cutoff energy have been found. The condition for the emergence of regions of multiflux ion flows with the formation of collisionless shock waves has been investigated, the spatial boundaries of the regions have been determined, and the moment of the onset of such a regime has been indicated. The main conclusion that follows from the above analysis is the difference in the behaviour of ions in the axial region of the tubular beam, enclosed between the laser intensity maximum and the beam axis, and in the off-axis region located at larger radii than the position of the intensity maximum. After the breaking of the ion flux in the off-axis region, three-flux and single-flux regimes of ion expansion are formed and subsequently retained. A different situation develops in the axial region, where, after the breaking of the ion flux, the ions flying towards the axis form single- and three-flux regions, and even five-flux regions after reflection from the axis. Obviously, over time, this picture becomes more complicated: after the reflected ions stop and start returning, one should expect the appearance of regions of a seven-flux flow. Then, the movement of ions in the paraxial region will become completely chaotised. An estimate has been obtained for the deceleration time of ions and the cumulation time on the axis, as well as an estimate for the characteristic period of ion oscillations near the beam axis and its dependence on the plasma and beam parameters.

The results presented in this work are based on the axial symmetry of a tubular relativistic laser beam, which implies its stability with respect to filamentation, resulting in the formation of a small-scale filamentary structure of the laser beam and the destruction of axial symmetry. A simple condition for the absence of relativistic filamentation can be written in the form of an inequality requiring that the characteristic thickness of the laser beam tube $\sim R$ does not exceed the characteristic wavelength of filamentation instability $2\pi\gamma/\omega_{Le}$, that is, $R/\lambda_{las} \lesssim \gamma\sqrt{n_{cr}/n_e}$. Here λ_{las} is the laser wavelength; n_e is the electron density of the medium; n_{cr} is the critical density; and $\gamma = \sqrt{1 + a_0^2/2}$. For the above discussed plasma and beam parameters ($n_{cr}/n_e \approx 10, \gamma \approx 3, R/\lambda_{las} \approx 1$) this inequality is satisfied with a large margin.

A more rigorous approach to the analysis of the filamentation instability of a relativistic laser beam with allowance for the relativistically ponderomotive nonlinearity, supplemented by numerical simulation [29], shows that the development of filamentation instability is determined by the relationship between two dimensionless parameters that characterise the laser-plasma system (at least for a cylindrical beam, the intensity of which decreases monotonically with increasing r and has a maximum on the axis), namely: $\mu \equiv R_{las}\omega_{Le}/c$ and $\eta \equiv P_0/P_{cr}$. Here $P_{cr} \approx 1.6198 \times 10^{10}\ (\omega/\omega_{Le})^2$ W is the critical power, and P_0 is the maximum power in the incident laser beam. As follows from [29], the region of stable (without filamentation) beam propagation includes all $\eta > 1$ if the value of μ is close to the value corresponding to the lowest self-trapped mode in the nonlinear regime, $\mu \approx \mu_e \sim 2$. On the other hand, filamentation also does not occur in a wide range of changes in μ for moderate values $1 < \eta \leqslant 10$. In fact, this means that the filamentation zone approximately corresponds to the region $\mu > 20, \eta > 16$ on the plane of parameters $\{\mu, \eta\}$, which indicates a wide range of applicability of our results. For the model of a tubular beam, instead of μ, one should use $\mu_{tr} = R\omega_{Le}/c$, that is, replace R_{las} by R. Note that the above simple condition for the absence of filamentation agrees with the results of a more rigorous consideration based on [29], if as η and μ we choose their smallest values, η_{min} and μ_{min}, corresponding to the point closest to the origin with coordinates $\{\eta_{min}, \mu_{min}\}$ at the boundary of the filamentation zone.

The model of cylindrical cumulation of ions on the axis is of interest as applied to a pulsed neutron source when initiating a fusion reaction, the idea of creating which was formulated back in the 1960s [30]. Since the reaction rate is proportional to the product of the densities of colliding particles and the cumulation over the laser focal spot size occurs quickly, one can expect to obtain a very short-pulse source of thermonuclear neutrons using a sufficiently dense (albeit transparent) plasma using the already available laser pulses of subpicosecond duration of relativistic intensity. In this case, we are not talking about an extremely high intensity, but one that provides deuteron energies at a level of less than 1 MeV, which corresponds to the parameter $a \lesssim 1$. The duration of a neutron burst will be determined by the transit time of a laser pulse through a self-focusing channel, $\tau_n = L_D/c$, the length of which is determined by the losses of a laser pulse [31], $L_D \approx ac\tau_{las}n_{cr}/4n_e$, where τ_{las} is the laser pulse duration.

For a tubular beam, the number of ions accelerated in the paraxial region and the number of ions accelerated in the off-axis region are approximately the same, and the maximum energies of the accelerated ions are also approximately equal. However, the cumulation effect leads to the fact that the values of the density of accelerated ions in the paraxial and off-axial regions are different, and, therefore, yields different values of the number N (per unit length of the laser channel) of the accelerated ions participating in the reaction (for example, deuterons). An estimate of this number can be obtained from the equation

$$\frac{dN}{dt} = \sigma(v)vN_d n_d. \tag{25}$$

Here N_d is the number of deuterons participating in the reaction with the cross section $\sigma(v)$ (per unit length of the laser channel), and n_d is the deuteron density.

For deuterons flying outward (in the off-axis region), the reaction time $t_{out} \approx l_d/v$ is specified by the path length l_d of accelerated deuterons with a velocity v in a gas of deuterons with an unperturbed density $n_d^+ = n_0$. Then for the number of dd-reactions (generated neutrons) from outward flying deuterons (as indicated by the superscript +), we obtain the estimate:

$$N_{out} \approx \sigma(v) l_d N_d^+ n_0. \tag{26}$$

For a plasma of subcritical density, the deuteron free path significantly exceeds the size of the focal laser spot, $l_d \gg R_{las}$. Indeed, according to [32], for the parameters of laser radiation and plasma discussed here, the value of l_d is $\sim$0.539 cm at deuteron energies $E_{max} = 200$ keV, $\sim$0.873 cm at 400 keV, and

~1.84 cm at 1 MeV, so that the above condition is satisfied with a large margin.

For deuterons flying towards the beam axis, two time intervals should be distinguished with significantly different neutron generation rates. The first corresponds to the characteristic time of flight t_c of accelerated deuterons with a velocity v in a gas of deuterons with an unperturbed density $n_d^- \approx n_d^+ \approx n_0$. Then, for the number of neutrons generated by deuterons flying inward (as indicated by the superscript '–') during the time $0 < t < t_c$, we obtain the estimate:

$$N_{in}^{t_c} \approx \sigma(v) v t_c N_d^- n_0. \quad (27)$$

Since the number of deuterons accelerated towards the axis, N_d^-, and to the outer region, N_d^+, are approximately equal, $N_d^- \approx N_d^+$, and are also equal to the gas density of unperturbed deuterons, $n_d^- \approx n_d^+ \approx n_0$, the difference between estimates (27) and (26) consists only in replacing t_c by t_{out}, which yields a significantly lower (by a factor of l_d/R_{las}) value of the number of neutrons, $N_{in}^{t_c}/N_{out} \approx R_{las}/l_d \ll 1$.

A much larger contribution should be expected from the effect of cumulation on the axis of two interpenetrating fluxes of accelerated deuterons with a relative velocity $2v$ and a density n_d^{pl} much higher than n_0. The characteristic time of neutron generation, which occurs at $t > t_c$, turns out to be of the order of the time of flight of deuterons t_{pl} through the central region of a 'compressed' plasma filament with a characteristic transverse size of $2R_{pl}$, that is, $t_{pl} \approx 2R_{pl}/v$. At $R_{pl} \ll R_{las}$, the time of flight of a deuteron through the region of a dense plasma filament, that is, the time of a neutron burst, is small compared to the time of cumulation on the axis ($t_c \gg t_{pl}$). To estimate the value of n_d^{pl}, we replace the real inhomogeneous distribution of the density of deuterons in a plasma filament with a singularity on the axis by an averaged one with a constant density, which can be found from the condition of conservation of the number of deuterons emitted from the ring region $R_{low} < r < R_{las}$, where $R_{low} = R[b + y_{low}(t_c)]$, into the axial region $0 < r < R_{pl}$,

$$n_d^{pl} = n_0 (R_{las}/R_{pl})^2 [1 - (R_{low}/R_{las})^2]. \quad (28)$$

As follows from the results of our numerical calculations (see Fig. 3), ions accelerated from the adjacent inner region of the ring are concentrated not only in the region of the plasma filament, but also in the rest of the inner region. This means that formula (28) gives a somewhat overestimated, but correct in order of magnitude, estimate of the deuteron density in the plasma filament. For the number of neutrons generated in a compressed plasma filament over time t_{pl}, we obtain the estimate:

$$N_{in}^{t_{pl}} \approx 2\sigma(2v) v t_{pl} N_d^- n_d^{pl}. \quad (29)$$

Using the ratio of (29) to (27),

$$\frac{N_{in}^{t_{pl}}}{N_{in}^{t_c}} = \frac{4\sigma(2v)}{\sigma(v)} \frac{R_{las}}{R_{pl}} \left[1 - \left(\frac{R_{low}}{R_{las}}\right)^2\right], \quad (30)$$

we can estimate the role of contributions to N_{in} from the neutron burst in the plasma filament and from the generation of neutrons in the volume from R_{pl} to R_{low}. For example, for the parameters $R_{low}/R_{las} \approx 0.645$ and $R_{las}/R_{pl} \approx 10^2$ discussed here, we obtain $N_{in}^{t_{pl}}/N_{in}^{t_c} \approx 2.4 \times 10^2 [\sigma(2v)/\sigma(v)] \gg 1$, taking into account the relatively weak dependence of the reaction cross section on the rate of deuterons in the range of interest near the value of $E_{max} \sim 1$ MeV [the ratio $\sigma(2v)/\sigma(v)$ is 1.935, 549, and 1.37 at the deuteron energy $E_{max} = 200$ keV, 400 keV, and 1 MeV, respectively]. Thus, the number of neutrons generated in a burst on the axis significantly exceeds the number of neutrons generated during the cumulation time t_c of deuterons on the axis. Note that the number of neutrons produced during the same time in the outer region is approximately equal to $N_{in}^{t_c}$ and, therefore, is also small in comparison with the number of neutrons in the burst. However, the total number of neutrons generated in the outer region during the time t_{out} is l_d/R_{las} times greater than $N_{in}^{t_c}$, which gives an estimate for the ratio $N_{in}^{t_{pl}}/N_{out} \approx 2.4 \times 10^2 (R_{las}/l_d)[\sigma(2v)/\sigma(v)]$. Taking into account the dependence of the reaction cross section and the deuteron mean free path on their velocity, that is, on the energy, we present the characteristic values of this ratio at different deuteron energies. For the upper limit of the discussed energy range $E_{max} = 1$ MeV, which corresponds to an intensity of 2×10^{19} W cm^{-2}, this ratio is $N_{in}^{t_{pl}}/N_{out} \approx 0.179$. With decreasing ion energy, this ratio increases: at $E_{max} = 0.4$ MeV, which corresponds to an intensity of 5.42×10^{18} W cm^{-2}, we obtain $N_{in}^{t_{pl}}/N_{out} \approx 0.426$, and at $E_{max} = 0.2$ MeV, which corresponds to an intensity of 2.33×10^{18} W cm^{-2}, we have $N_{in}^{t_{pl}}/N_{out} \approx 0.861$, that is, the quantities $N_{in}^{t_{pl}}$ and N_{out} become of the same order of magnitude. Finally, we present an estimate of the number of neutrons in the burst (per unit length of the laser channel):

$$N_{in}^{t_{pl}} = 4\sigma(2v) N_d^- n_0 \frac{R_{las}^2}{R_{pl}} \left[1 - \left(\frac{R_{low}}{R_{las}}\right)^2\right]. \quad (31)$$

For deuterons with energy $E_{max} = 0.2$ MeV, we have $\sigma(2v) \approx 0.0728 \times 10^{-24}$ cm^2 and for the rest of the plasma and beam parameters used above [$n_0 = 10^{20}$ cm^{-3}, $R_{las} = 10^{-3}$ cm, $R_{pl} = 10^{-5}$ cm, $N_d^- = \pi n_0 R_{las}^2 (1 - R_{low}^2/R_{las}^2) \approx 0.6\pi \times 10^{14}$ cm^{-1}] we obtain $N_{in}^{t_{pl}} \approx 3.3 \times 10^8$ cm^{-1}.

In this work, we have theoretically substantiated the phenomenon of cumulative laser generation of neutrons in the form of a short (compared to standard methods) burst that occurs when ion fluxes intersect during their cylindrical cumulation, which is consistent with numerical calculations. We emphasize that the very short duration of the neutron pulse turns out to be important, with practically no loss in the number of generated thermonuclear neutrons in comparison with the usually discussed scheme of their generation from the axis of the laser beam in the volume of the surrounding gas [9]. Usually, the time t_{pl} is short in comparison with the time τ_n, and the latter determines the duration of the neutron burst, which, for example, for a laser pulse of moderate intensity, $a \sim 1$, with a duration of ~400 fs, propagating in a plasma with $n_0 = 10^{20}$ cm^{-3}, will be $\tau_n = a\tau_{las} n_{cr}/4n_e \approx 5$ ps. In this case, the yield of dd-neutrons per burst is expected at a level of $\sim 0.5 \times 10^7$. A neutron source of ultrashort duration may be of interest for diagnosing fast processes in dense substances.

Acknowledgements. This work was supported by the Russian Science Foundation (Grant No. 17-12-01283).

References

1. Sarkisov G.S., Bychenkov V.Yu., Tikhonchuk V.T., Maksimchuk A., Chen S.-Y., Wagner R., Mourou G., Umstadter D. *JETP Lett.*, **66**, 828 (1997) [*Pis'ma Zh. Eksp. Teor. Fiz.*, **66**, 787 (1997)].
2. Sarkisov G.S., Bychenkov V.Yu., Tikhonchuk V.T. *JETP Lett.*, **69**, 20 (1999) [*Pis'ma Zh. Eksp. Teor. Fiz.*, **69**, 20 (1999)].

3. Sarkisov G.S., Bychenkov V.Yu., Novikov V.N., Tikhonchuk V.T., Maksimchuk A., Chen S.-Y., Wagner R., Mourou G., Umstadter D. *Phys. Rev. E*, **59**, 7042 (1999).
4. Tripathi V.K., Taguchi T., Liu C.S. *Phys. Plasmas*, **12**, 043106 (2005).
5. Lifschitz A., Sylla F., Kahaly S., Flacco A., Veltcheva M., Sanchez-Arriaga G., Lefebvre E., Malka V. *New J. Phys*., **16**, 033031 (2014).
6. Macchi A., Ceccherini F., Cornolti F., Kar S., Borghesi M. *Plasma Phys. Control. Fusion*, **51**, 024005 (2009).
7. Kovalev V.F., Bychenkov V.Yu. *Plasma Phys. Rep.*, **41**, 343 (2015) [*Fiz. Plazmy*, **41**, 374 (2015)].
8. Kovalev V.F., Bychenkov V.Yu. *J. Exp. Theor. Phys.*, **121** (1), 1 (2015) [*Zh. Eksp. Teor. Fiz*., **148** (1), 5 (2015)].
9. Bychenkov V.Yu., Tikhonchuk V.T., Tolokonnikov S.V. *J. Exp. Theor. Phys*., **88** (6), 1137 (1999) [*Zh. Eksp. Teor. Fiz*., **115**, 2080 (1999)].
10. Yamagiwa M., Koga J. *J. Phys. D: Appl. Phys*., **32**, 2526 (1999).
11. Fritzler S., Najmudin Z., Malka V., Krushelnick K., Marle C., Walton B., Wei M.S., Clarke R.J., Dangor A.E. *Phys. Rev. Lett.*, **89**, 165004 (2002).
12. d'Humieres E., Antici P., Glesser M., Boeker J., Cardelli F., Chen S., Feugeas J.L., Filippi F., Gauthier M., Levy A., Nicolai P., Pepin H., Romagnani L., Sciscio M., Tikhonchuk V.T., Willi O., Kieffer J.C., Fuchs J. *Plasma Phys. Control. Fusion*, **55**, 124025 (2013).
13. Zani A., Dellasega D., Russo V., Passoni M. *Carbon*., **56**, 358 (2013).
14. Kuznetsov A.V., Esirkepov T.Zh., Kamenets F.F., Bulanov S.V. *Fiz. Plazmy*, **27**, 225 (2001).
15. Pukhov A., Sheng Z.-M., Meyer-ter-Vehn J. *Phys. Plasmas*, **6**, 2847 (1999).
16. Popov K.I., Rozmus W., Bychenkov V.Yu., Naseri N., Capjack C.E., Brantov A.V. *Phys. Rev. Lett*., **105**, 195002 (2010).
17. Bochkarev S.G., Brantov A.B., Gozhev D.A., Bychenkov V.Yu. *J. Russ. Laser Res.*, **42**, 292 (2021).
18. Pradhan P., Ung B. *IEEE Photonics J*., **10** (1), 6500310 (1999).
19. Balakirev V.A., Onishenko I.N., Povrozin A.I., Tolstoluzhsky A.P., Yegorov A.M. *IEEE Trans. Plasma Sci*., **36** (4), 1847 (2008).
20. Schimpf D.N., Putnam W.P., Grogan M.D.W., Ramachandran S., Kartner F.X. *Opt. Express*, **21** (15), 18469 (2013).
21. Girgel S.S. *Probl. Fiz. Mat. Tekh*., No. 4 (25), 11 (2015).
22. Balakirev V.A., Onishchenko I.N., Povrozin A.I., Tolstoluzhsky A.P., Egorov A.M. *Vopr. At. Nauki Tekh*., **4**, 77 (2008).
23. Miller M.A. *Izv. Vyshch. Uchebn. Zaved., Ser. Radiofiz*., **1**, 110 (1958).
24. Litvak A.G., in *Voprosy teorii plazmy* (Problems of the Theory of Pplasma) Ed. by M.A. Leontovich (Moscow: Atomizdat, 1980) Vol. 10, pp 164–242.
25. Kaplan A.E., Dubetsky B.Y., Shkolnikov P.L. *Phys. Rev. Lett.*, **91** (14), 143401 (2003).
26. Arnold V.I. *Catastrophe Theory* (Berlin: Springer-Verlag, 1984; Moscow: Nauka, 1990).
27. Gurevich A.V., Zybin K.P. *Usp. Fiz. Nauk*, **165** (7), 723 (1995).
28. Kovalev V.F., Popov K.I., Bychenkov V.Yu., Rozmus W. *Phys. Plasmas*, **14**, 052103 (2007).
29. Borisov A.B., Shiryaev O.B., McPherson A., Boyer K., Rhodes C.K. *Plasma Phys. Control. Fusion*, **37**, 569 (1995).
30. Gryzinski M., Nowikowski J., Sadowski M., Skladnik-Sadowska E., Suckewer S. *Plasma Phys. Control. Fusion*, **10**, 450 (1968).
31. Decker C.D., Mori W.B., Tzeng K.C., Katsouleas T. *Phys. Plasmas*, **3**, 2047 (1996).
32. Grigoriev I.S., Meilikhov E.Z. (Eds) *Handbook of Physical Quantities* (Boca Raton: CRC Press, 1997; Moscow: Energoatomizdat, 1991).